

Superconductivity in two-dimensional phosphorus carbide (β_0 -PC)

Bao-Tian Wang,^{1,2,*} Peng-Fei Liu,^{1,2,†} Tao Bo,^{1,2} Wen Yin,^{1,2} and Fangwei Wang^{2,3}

¹*Institute of High Energy Physics, Chinese Academy of Sciences (CAS), Beijing 100049, China*

²*Dongguan Institute of Neutron Science (DINS), Dongguan 523808, China*

³*Beijing National Laboratory for Condensed Matter Physics, Institute of Physics, Chinese Academy of Sciences (CAS), Beijing 100080, China*

Two-dimensional (2D) boron has been predicted to show superconductivity. However, intrinsic 2D carbon and phosphorus have not been reported to be superconductors, which, inspires us to seek superconductivity in their mixture. Here we perform first-principles calculations of the electronic structure, phonon dispersion, and electron-phonon coupling of the metallic phosphorus carbide monolayer, the β_0 -PC. Results show that it is an intrinsic phonon-mediated superconductor, with estimated superconducting temperature T_c to be ~ 13 K. The main contribution to the electron-phonon coupling is from the out-of-plane vibrations of phosphorus. A Kohn anomaly on the first acoustic branch is observed. The superconducting related physical quantities is found tunable by applying strain or carrier doping.

PACS numbers: 73.20.-r, 74.70.Ad, 71.15.Mb,

Owing to the developments of the atomic techniques, like molecular beam epitaxy [1], atomic layer deposition [2], pulsed laser deposition [3], magnetron sputtering [4], etc., many two-dimensional (2D) or layered superconductors have been synthesized successfully [5, 6]. The superconductivity can be remarkably robust in the 2D limit with respect to the corresponding parental bulk materials [7, 8]. The fascinating phenomena of the competition with charge density waves [9], the Kohn anomaly [10], and the strong spin-orbit coupling [11] for superconductivity in 2D systems have attracted many attentions.

Since the well-known discovery of graphene by mechanical exfoliation [12, 13], various 2D-monolayer carbon [14, 15] and phosphorus [16, 17] have been successfully obtained. Both graphene and phosphorene can be manipulated to be superconductors through carrier doping [18–21], strain [18, 22], and/or metal-decorating/intercalating [23–27]. However, till now, no superconducting properties have been experimentally observed or theoretically predicted for these famous 2D materials in their intrinsic forms. This fact stimulates our interests to seek superconducting state in their compounds, *i.e.* the 2D phosphorus carbide (PC).

Recently, various allotropes of 2D-monolayer PC were theoretically predicted [28, 29] to be stable through the particle-swarm optimization method [30] and the density functional theory (DFT) [31]. Later on, few-layer 2D black PC has been synthesized successfully via a novel carbon doping technique [32]. Among all reported 2D PC, only the graphene-like β_0 -PC exhibits metallic character [28, 33] and has been testified carefully to be stable in a DFT level [33]. Therefore, it is necessary to verify whether this newly reported phase exhibits superconductivity or not.

The calculations are performed at the DFT level, employing the local density approximation and norm-conserving pseudopotentials [34, 35] as implemented in the QUANTUM-

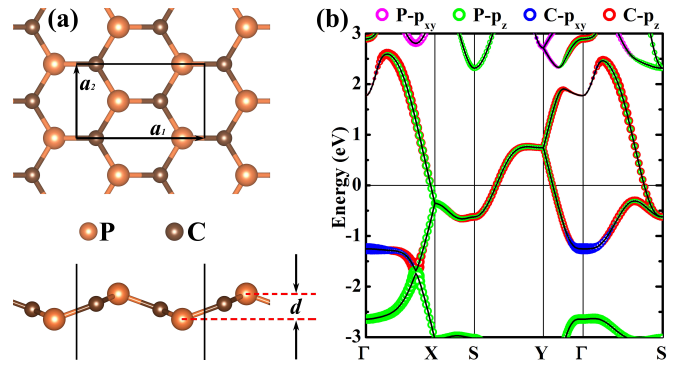


FIG. 1: Crystal and band structures of β_0 -PC. (a) Schematic of the crystal structure with the unit cell indicated by the black rectangle. a_1 and a_2 are the lattice constants while d stands for the buckling thickness. (b) Orbital-resolved band structure with the contributions of p_{xy} and p_z orbitals of P (C) atoms being indicated by magenta and green (blue and red) hollow circles, respectively. The Fermi energy level is set at zero.

ESPRESSO (QE) package [36]. The plane-waves kinetic-energy cutoff is set as 100 Ry and the structural optimization is performed until the forces on atoms are less than 10 meV/Å. Monolayer PC is simulated with a vacuum thickness of 20 Å, which is enough to decouple the adjacent layers. An unshifted Brillouin-zone (BZ) \mathbf{k} -point mesh of 16×6 and a Hermitian-Gaussian smearing method are adopted for the electronic charge density calculations. The phonon modes are computed within density-functional perturbation theory [37] on a 8×3 \mathbf{q} mesh.

The optimized phosphorus carbide (β_0 -PC) monolayer crystallizes in the polar orthorhombic structure with space group $Pmn21$ (no. 31), showing the C_{2v} symmetry. Similar to the planar honeycomb lattice of graphene [12, 13], all the atoms in the unit cell of β_0 -PC are 3-fold coordinated, which endows the structure with topologically repeated hexagonal configuration. According to the chemical octet rule [38], C atoms usually feature p -electron conjugated bonds via sp^2 -

*E-mail: wangbt@ihep.ac.cn

†E-mail: pfliu@ihep.ac.cn

hybridization in the planar geometry (*e.g.*, graphene [12, 13], graphenylene [39, 40], and phagraphene [41]), whereas P atoms adopt sp^3 -hybridization with a lone electron pair forming the puckered configuration of phosphorene [42, 43]. As shown in Figure 1a, the alternating manner of P and C atoms renders β_0 -PC monolayer a buckled structure, which mainly stems from the competition between the favoured planar sp^2 -hybridization of C atoms and nonplanar sp^3 -hybridization of P atoms. β_0 -PC monolayer shows an anisotropic rectangular structure with lattice constants $a_1=4.99$ Å and $a_2=2.87$ Å ($a_1/a_2 \approx 1.74$), respectively, which are consistent with reported results of $a_1=5.02$ Å and $a_2=2.95$ Å ($a_1/a_2 \approx 1.70$) [33]. The buckling thickness of the β_0 -PC monolayer, simply measured by the distance between the top and bottom atomic layers, is $d=0.98$ Å being slightly smaller than that (1.24 Å) in the honeycomb lattice of semiconducting blue phosphorene [44]. Our QE calculations reveals two distinct types of P-C bond lengths varying from 1.72 Å to 1.74 Å for β_0 -PC monolayer, which are in analogy with the reported values (1.75 Å and 1.77 Å) [33] obtained by VASP [31, 45] and different from one P-C bond length of 1.78 Å [28] using SIESTA [46]. The P-C bond lengths in β_0 -PC monolayer are between the P-C single bond length (1.83 Å) and the P-C double bond length (1.67 Å) [33, 47], indicating some greater p -character sp^2 -hybridization for C atoms and some less p -character sp^3 -hybridization for P atoms, which helps stabilize the anisotropic buckled rectangular lattice [33].

The orbital-resolved band structure of β_0 -PC is shown in Figure 1b. β_0 -PC monolayer exhibits intrinsic metallic features with bands crossing the Fermi level, which is in good agreement with the previous theoretical calculations [28, 33]. In the vicinity of Fermi level, the valence and conduction bands mostly originate from the hybridization of P- p_z and C- p_z orbitals according to the partial band projections. Thus, they come into being a high density of 2D π -electron gas at the Fermi level via unconventional π - π interactions which delocalize the lone pair electrons of P atoms and bring the imperfect sp^2 - and sp^3 -hybridized states for β_0 -PC monolayer. Apparently, such characteristic gives rise to metallic behavior for β_0 -PC monolayer, and accordingly, favours a superconducting sheet.

We now focus on the vibration properties and the electron-phonon coupling (EPC) in β_0 -PC. Figure 2a shows the phonon dispersion over the whole BZ. The absence of the imaginary modes clearly indicates that the β_0 -PC is dynamically stable. Our results agree well with one recent calculation [33] by Rajbanshi *et al.* who use the finite displacement method in obtaining phonon spectra. From the decomposition of the phonon spectrum with respect to C and P atomic vibrations, as indicated in Figure 2a, we find that the main contribution to the acoustic branches below 150 cm^{-1} is the phosphorus out-of-plane P_z vibrations. The interaction between P and C atoms contributes to the intermediate-frequency region from 150 to 634 cm^{-1} . The in-plane modes of C atoms occupy the high frequencies above 860 cm^{-1} . Similar to Li-decorated monolayer graphene [25] and 2D Cu-benzenehexathial (Cu-BHT) [48], here, the vertical vibrations of C atoms are also lower than their horizontal modes.

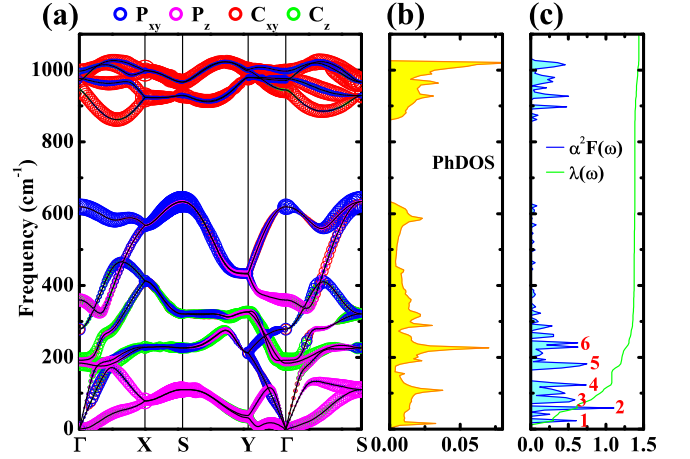


FIG. 2: (a) Phonon frequency dispersion of β_0 -PC weighted by the motion modes of P and C atoms. The blue, magenta, red, and green hollow circles indicate P horizontal, P vertical, C horizontal, and C vertical modes, respectively. (b) PhDOS and (c) Eliashberg spectral function $\alpha^2 F(\omega)$ and cumulative frequency-dependent of EPC $\lambda(\omega)$. The peaks of $\alpha^2 F(\omega)$ are numbered by vibration frequency from 1 to 6.

The phonon density of state (PhDOS), the Eliashberg electron-phonon spectral function $\alpha^2 F(\omega)$, and the cumulative frequency-dependent of EPC $\lambda(\omega)$ are displayed in Figures 2b and 2c. Here, the $\alpha^2 F(\omega)$ and the $\lambda(\omega)$ are calculated by

$$\alpha^2 F(\omega) = \frac{1}{2\pi N(E_F)} \sum_{q\nu} \frac{\gamma_{q\nu}}{\omega_{q\nu}} \delta(\omega - \omega_{q\nu}) \quad (1)$$

and

$$\lambda(\omega) = 2 \int_0^\omega \frac{\alpha^2 F(\omega')}{\omega'} d\omega', \quad (2)$$

where $N(E_F)$ is the electronic density of state at the Fermi level and $\gamma_{q\nu}$ is the phonon linewidth. We find that the low-frequency phonons, mainly associated with the out-of-plane P_z modes, are key to achieving a high EPC in β_0 -PC as they account for 1.08 (73%) of the total EPC ($\lambda=1.48$). As shown in Figure 2c, the 1st to 4th peaks of the $\alpha^2 F(\omega)$ are responsible for this part. The 5th and the 6th peaks hold the main feature of the out-of-plane C_z modes and associate with a EPC strength of 0.23 (16%). Similar to graphene [18] and 2D Cu-BHT [48], the EPC induced by high-frequency phonons is almost negligible. Specifically, the high-frequency phonons, mainly the C_{xy} modes, only contribute 0.06 (4%) of the total EPC. Overall, our calculated EPC value of 1.48 clearly makes the 2D β_0 -PC an intermediate to strong conventional superconductor.

The Fermi surface contour of β_0 -PC is shown in Figure 3a, where one can see one electron pocket centered at the Y point. Away from the Γ point and along S-X-S, a hole arc is emerged. Along Y-S and near the S point, the electron pocket crosses with the hole arc. Given the electronic states of P and C atoms at the Fermi level, the out-of-plane phonon vibrations couple

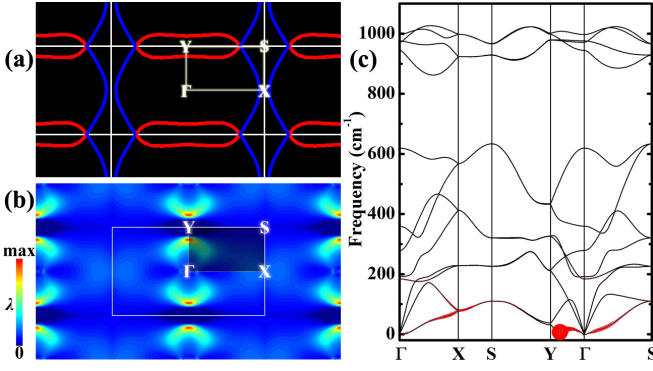


FIG. 3: (a) Fermi surface in BZ with hole and electron bands being indicated by red and green contour lines, respectively. (b) The distribution of \mathbf{q} -resolved EPC $\lambda_{\mathbf{q}}$ for the first transverse acoustic branch in BZ. (c) Phonon spectrum with the size of red dots being drawn proportional to the magnitude of the EPC $\lambda_{q\nu}$.

TABLE I: The superconductive parameters of μ^* , $N(E_F)$ (in unit of states/spin/Ry/cell), ω_{\log} (in K), λ , and T_c (in K) for some intrinsic 2D-monolayer-phonon-mediated superconductors.

Compounds	μ^*	$N(E_F)$	ω_{\log}	λ	T_c	Refs.
B ₂ C	0.1		314.8	0.92	19.2	[58]
B Δ /B \square /B \diamond	0.1			1.1/0.8/0.6	21/16/12	[54]
B (α sheet)	0.05	5.85	262.2	0.52	6.7	[57]
B (β_{12})	0.1-0.15	8.12	425	0.69	14	[55]
TiSi ₄	0.1			0.59	5.8	[59]
Li ₂ B ₇	0.12		462.8	0.56	6.2	[60]
Mo ₂ C	0.1			0.63	5.9	[56]
Cu-BHT	0.1		51.8	1.16	4.43	[48]
β_0 -PC	0.1	7.27	118.0	1.48	13.35	This work

strongly with the 2D π -electron hybridization of P- p_z and C- p_z . As a result, the distribution of the $\lambda_{\mathbf{q}}$ ($\lambda_{q\nu} = \frac{\gamma_{q\nu}}{\pi\hbar N(E_F)\omega_{q\nu}^2}$) for the first transverse acoustic (TA) branch in BZ should overlap with the electronic Fermi surface. In Figure 3b, an arc-type distribution of $\lambda_{\mathbf{q}}$ is observed and is believed to strongly couple with the electron pocket near the Y point. Combined Figure 3b with Figure 3c, one can find that the largest value of the EPC appears at $\mathbf{q}_1=(0,0.36)$ point along Γ -Y on the first TA branch. This Kohn anomaly [49, 50] or softening of the phonon mode yields significant coupling between electrons and acoustic phonons, with a very low frequency of $\sim 8 \text{ cm}^{-1}$.

Using our calculated Eliashberg spectral function $\alpha^2F(\omega)$ and λ , we calculate the logarithmic average frequency defined as $\omega_{\log} = \exp\left[\frac{2}{\lambda} \int_0^\infty \frac{d\omega}{\omega} \alpha^2F(\omega)\right]$ to be 118.0 K. Using a typical value of the effective screened Coulomb repulsion constant $\mu^*=0.1$, the superconducting transition temperature T_c can be estimated, according to the Bardeen-Cooper-Schrieffer (BCS) theory [51], by the Allen-Dynes modified McMillan

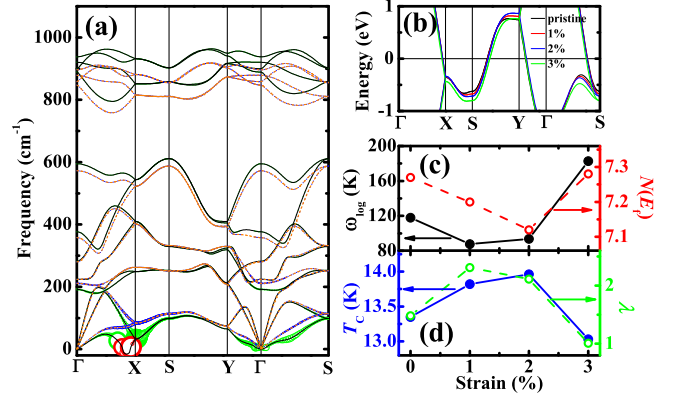


FIG. 4: Superconducting related physical quantities under equibiaxial strain. (a) Phonon spectra under strain of 2% (solid black lines) and 3% (dashed orange lines). The sizes of green/red and blue circles are drawn proportional to the magnitude of the EPC $\lambda_{q\nu}$ for strain of 2% and 3%, respectively. The red circles have been reduced 20-fold. (b) Band structures. The Fermi energy level is set at zero. (c) ω_{\log} and $N(E_F)$ as well as (d) T_c and λ under strain. The lines in (c) and (d) are only guides to the eye.

equation [52, 53]

$$T_c = \frac{\omega_{\log}}{1.2} \exp \left[-\frac{1.04(1 + \lambda)}{\lambda - \mu^*(1 + 0.62\lambda)} \right]. \quad (3)$$

Our calculated value of T_c is 13.35 K, comparable with that predicted in 2D Boron [54, 55].

Actually, superconductivity has little been predicted for intrinsic 2D-monolayer systems. In Table I, we list the superconductive parameters of μ^* , $N(E_F)$, ω_{\log} , λ , and T_c for some typical 2D phonon-mediated superconductors [48, 54–60]. All these systems have been predicted to appear superconductivity without external conditions of high pressure, strain, carrier doping, metal decorations/intercalations, and/or functional groups. It is clear that the T_c of β_0 -PC is larger than that of 2D boron (α sheet) [57], TiSi₄ [59], Li₂B₇ [60], Mo₂C [56], and Cu-BHT [48] while smaller than that of B₂C [58] and B Δ [54]. Among these systems, β_0 -PC exhibits the largest value of λ but holds a relatively small value of ω_{\log} . The vertical vibrations of P atoms in β_0 -PC play similar role in EPC as that of S atoms in Cu-BHT [48].

We note that the 2D boron sheets have been successfully grown on the Ag(111) substrate [61, 62]. Growing β_0 -PC on different substrates may also be realized in experiments. In one recent calculation [33], strain was found can modulate the electronic structure and phonon spectrum of β_0 -PC. Here, we want to know the strain effects on the superconductivity, as already known critical for graphene and phosphorene [18, 22]. Under tensile equibiaxial strain of $0\% \leq \varepsilon \leq 3\%$ where $\varepsilon = \frac{a-a_0}{a_0} \times 100\%$, the atomic structures are fully relaxed. Most of our calculated phonon dispersions are positive. These results agree well with previous study [33] where the β_0 -PC was found dynamically stable up to 9.1% strain. We show in Figure 4a the phonon dispersions together with the magnitude of the EPC $\lambda_{q\nu}$ under strains of 2% and 3%. We find that the

Kohn anomaly point under strain of 2% (with some imaginary frequencies) is moved from near the Y point along Γ -Y (under strain of 0% and 1%) to near the X point along Γ -X. The EPC λ_{qv} at the Kohn anomaly point is extremely large. Upon further tensile strain up to 3%, the Kohn anomaly point over the whole BZ disappears; the phonon frequencies below 300 cm^{-1} are strengthened while that above 300 cm^{-1} are lowered down; the EPC λ_{qv} becomes small.

Under strain, the overall band structure (shown in Figure 4b) is shifted downward and the $N(E_F)$ (Figure 4c) is decreased firstly to ~ 7.1 States/spin/Ry/cell ($\varepsilon=2\%$) and then rebounded to ~ 7.3 ($\varepsilon=3\%$). Normally, the superconducting related physical quantities of ω_{\log} , λ , and T_c should increase or decrease monotonously along with applied strain [18, 55]. However, in our case, the ω_{\log} decreases firstly to ~ 90 K ($\varepsilon=1-2\%$) and then increases to 182.8 K at $\varepsilon=3\%$ (Figure 4c); the λ and T_c increase firstly and then decrease (Figure 4d). The abnormal behaviors of these physical quantities are tightly related to the existence of the Kohn anomaly points under strains of 0-2% where the EPC strengthens are extremely enlarged. Under $\varepsilon=3\%$, without the Kohn anomaly point, β_0 -PC still exhibits the superconducting properties of $\lambda=1.01$ and $T_c=13.03$ K. So, the superconducting behavior in β_0 -PC is robust.

Charge carrier doping can also modulate the electronic structure and phonon spectrum of materials [18–21, 63, 64]. In our present study, the carrier doping is simulated by using a jellium model, whereby the excess/defect electronic charge is compensated by a uniform neutralizing background [18–20, 63, 64]. Under different concentrations of the electron or hole doping, both the lattice constants and the atomic structures are fully relaxed. As shown in Figure 5, the electron doping (0.1 e/cell) can induce disappearance of the Kohn anomaly point, raise the phonon frequencies below 300 cm^{-1} a little up and lower down that above 300 cm^{-1} . As a result, the EPC λ_{qv} become small and the total λ is reduced to 0.96. Through electron doping, the overall band structure is shifted downward and the $N(E_F)$ is increased to ~ 7.5 States/spin/Ry/cell, the ω_{\log} is increased to 175 K, and the T_c is decreased to 11.56 K. Thus, the electron doping can suppress the superconducting transition temperature of β_0 -PC.

Under the condition of the hole doping, as indicated in Figure 5, the Kohn anomaly point near the Y point along Γ -Y is still evident. The phonon frequencies below (above) 300 cm^{-1} are lowered down (raised up) a little. As a result, the EPC λ_{qv} on the first acoustic branch are still large and the total λ are only reduced to 1.43 and 1.07 at doping levels of 0.1 and 0.2 h/cell, respectively. The overall band structures are shifted upward and the $N(E_F)$ are increased to ~ 7.6 and 8.0 States/spin/Ry/cell, the ω_{\log} are increased to 120 and 174 K, and the T_c are modulated to 13.09 and 13.47 K. These results

indicate that the hole doping, although changes the electronic structure and phonon spectrum of β_0 -PC to some extent, induces limited effects on the superconducting transition temperature.

In summary, we have investigated the structure, electronic structure, phonon spectrum, EPC, and superconducting properties of the phosphorus carbide monolayer (β_0 -PC) using

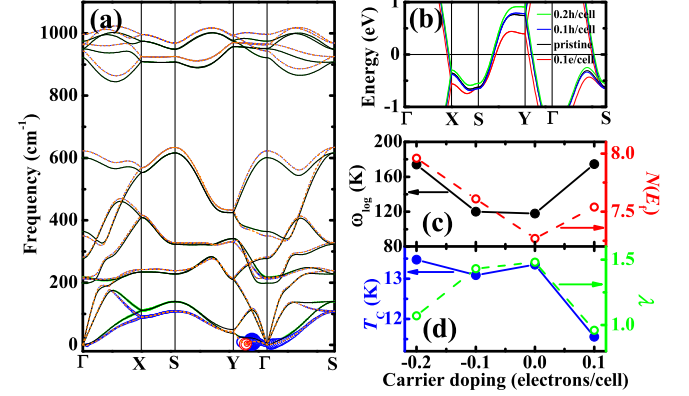


FIG. 5: Superconducting related physical quantities under carrier doping. (a) Phonon spectra under electron doping of 0.1 e/cell (solid black lines) and hole doping of 0.2 h/cell (dashed orange lines). The sizes of green and blue/red circles are drawn proportional to the magnitude of the EPC λ_{qv} for carrier doping of 0.1 e/cell and 0.2 h/cell, respectively. The red circles have been reduced 20-fold. (b) Band structures. The Fermi energy level is set at zero. (c) ω_{\log} and $N(E_F)$ as well as (d) T_c and λ under carrier doping. The lines in (c) and (d) are only guides to the eye.

first-principles calculations. We predicted that this intrinsic monolayer material, the first example within the 2D carbon and phosphorus families, is an intermediate conventional superconductor. The out-of-plane P_z vibrations together with the lone pair electrons of $P-p_z$ play dominant role for the EPC. The superconducting behavior in β_0 -PC is robust, even under conditions of tensile equibiaxial strain or electron doping the Kohn anomaly point has been suppressed. Our findings provide a new choice in realizing superconductor in 2D limit and will inspire further efforts in this field.

I. ACKNOWLEDGMENTS

This work was supported by National Natural Science Foundation of China under Grant Nos. 11675255 and 11374197.

[1] Chang, K.; Deng, P.; Zhang, T.; Lin, H. C.; Zhao, K.; Ji, S. H.; Wang, L. L.; He, K.; Ma, X. C.; Chen, X.; Xue, Q. K. Molecular Beam Epitaxy Growth of Superconducting LiFeAs Film on $\text{SrTiO}_3(001)$ Substrate. *EPL* **2015**, *109*, 28003.

[2] Klug, J. A.; Prpslier, T.; Elam, J. W.; Cook, R. E.; Hiller, J. M.; Claus, H.; Becker, N. G.; Pellin, M. J. Atomic Layer Deposition of Amorphous Niobium Carbide-Based Thin Film Superconductors. *J. Phys. Chem. C* **2011**, *115*, 25063-25071.

- [3] Shinde, S. R.; Ogale, S. B.; Greene, R. L.; Venkatesan, T.; Canfield, P. C.; Bud'ko, S. L.; Lapertot, G.; Petrovic, C. Superconducting MgB_2 Thin Films by Pulsed Laser Deposition. *Appl. Phys. Lett.* **2001**, *79*, 227-229.
- [4] Haberkorn, N.; Bengio, S.; Troiani, H.; Suárez, S.; Pérez, P. D.; Granell, P.; Golmar, F.; Sirena, M.; Guimpel, J. Thickness Dependence of The Superconducting Properties of $\gamma\text{-Mo}_2\text{N}$ Thin Films on Si (001) Grown by DC Sputtering at Room Temperature. *Mater. Chem. Phys.* **2018**, *204*, 48-57.
- [5] Uchihashi, T. Two-Dimensional Superconductors With Atomic-Scale Thickness. *Supercond. Sci. Technol.* **2017**, *30*, 013002.
- [6] Brun, C.; Cren, T.; Roditchev, D. Review of 2D Superconductivity: The Ultimate Case of Epitaxial Monolayers. *Supercond. Sci. Technol.* **2017**, *30*, 013003.
- [7] Ge, J. F.; Liu, Z. L.; Liu, C.; Gao, C. L.; Qian, D.; Xue, Q. K.; Liu, Y.; Jia, J. F. Superconductivity Above 100 K in Single-Layer FeSe Films on Doped SrTiO_3 . *Nature Mater.* **2014**, *14*, 285-289.
- [8] Clark, K.; Hassanien, A.; Khan, S.; Braun, K. F.; Tanaka, H.; Hla, S. W. Superconductivity in First Four Pairs of $(\text{BETS})_2\text{GaCl}_4$ Molecules. *Nat. Nanotechnol.* **2010**, *5*, 261-265.
- [9] Xi, X.; Zhao, L.; Wang, Z.; Berger, H.; Forró, L.; Shan, J.; Mak, K. F. Strongly Enhanced Charge-Density-Wave Order in Monolayer NbSe_2 . *Nature Nanotechnol.* **2015**, *10*, 765-770.
- [10] Yan, J. A.; Stein, R.; Schaefer, D. M.; Wang, X. Q.; Chou, M. Y. Electron-Phonon Coupling in Two-Dimensional Silicene and Germanene. *Phys. Rev. B* **2013**, *88*, 121403.
- [11] Nam, H.; Chen, H.; Liu, T.; Kim, J.; Zhang, C.; Yong, J.; Lemberger, T. R.; Kratz, P. A.; Kirtley, J. R.; Moler, K.; Adams, P. W.; MacDonald, A. H.; Shih, C. K. Ultrathin Two-Dimensional Superconductivity with Strong Spin-Orbit Coupling. *Proc. Natl Acad. Sci.* **2016**, *113*, 10513-10517.
- [12] Novoselov, K. S.; Geim, A. K.; Morozov, S.; Jiang, D.; Zhang, Y.; Dubonos, S.; Grigorieva, I.; Firsov, A. Electric Field Effect in Atomically Thin Carbon Films. *Science* **2004**, *306*, 666-669.
- [13] Novoselov, K.; Geim, A. K.; Morozov, S.; Jiang, D.; Katsnelson, M.; Grigorieva, I.; Dubonos, S.; Firsov, A. Two-Dimensional Gas of Massless Dirac Fermions in Graphene. *Nature* **2005**, *438*, 197-200.
- [14] Li, G.; Li, Y.; Liu, H.; Guo, Y.; Li, Y.; Zhu, D. Architecture of Graphdiyne Nanoscale Films. *Chem. Commun.* **2010**, *46*, 3256-3258.
- [15] Peng, Q.; Dearden, A. K.; Crean, J.; Han, L.; Liu, S.; Wen, X.; De, S. New Materials Graphyne, Graphdiyne, Graphone, and Graphane: Review of Properties, Synthesis, and Application in Nanotechnology. *Nanotechnol., Sci. Appl.* **2014**, *7*, 1-29.
- [16] Liu, H.; Neal, A. T.; Zhu, Z.; Luo, Z.; Xu, X.; Tománek, D.; Ye, P. D. Phosphorene: An Unexplored 2D Semiconductor with a High Hole Mobility. *ACS Nano* **2014**, *8*, 4033-4041.
- [17] Zhang, J. L.; Zhao, S.; Han, C.; Wang, Z.; Zhong, S.; Sun, S.; Guo, R.; Zhou, X.; Gu, C. D.; Yuan, K. D.; Li, Z.; Chen, W. Epitaxial Growth of Single Layer Blue Phosphorus: A New Phase of Two-Dimensional Phosphorus. *Nano Lett.* **2016**, *16*, 4903-4908.
- [18] Si, C.; Liu, Z.; Duan, W.; Liu, F. First-Principles Calculations on the Effect of Doping and Biaxial Tensile Strain on Electron-Phonon Coupling in Graphene. *Phys. Rev. Lett.* **2013**, *111*, 196802.
- [19] Margine, E. R.; Giustino, F. Two-Gap Superconductivity in Heavily n -Doped Graphene: *Ab initio* Migdal-Eliashberg Theory. *Phys. Rev. B* **2014**, *90*, 014518.
- [20] Shao, D. F.; Lu, W. J.; Lv, H. Y.; Sun, Y. P. Electron-Doped Phosphorene: A Potential Monolayer Superconductor. *EPL* **2014**, *108*, 67004.
- [21] Savini, G.; Ferrari, A. C.; Giustino, F. First-Principles Prediction of Doped Graphane as a High-Temperature Electron-Phonon Superconductor. *Phys. Rev. Lett.* **2010**, *105*, 037002.
- [22] Ge, Y.; Wan, W.; Yang, F.; Yao, Y. The Strain Effect on Superconductivity in Phosphorene: A First-Principles Prediction. *New J. Phys.* **2015**, *17*, 035008.
- [23] Ludbrook, B. M.; Levy, G.; Nigge, P.; Zonno, M.; Schneider, M.; Dvorak, D. J.; Veenstra, C. N.; Zhdanovich, S.; Wong, D.; Dosanjh, P.; Straß, C.; Stöhr, A.; Forti, S.; Ast, C. R.; Starke, U.; Damascelli, A. Evidence for Superconductivity in Li-Decorated Monolayer Graphene. *Proc. Natl. Acad. Sci. U.S.A.* **2015**, *112*, 11795-11799.
- [24] Margine, E. R.; Lambert, H.; Giustino, F. Electron-Phonon Interaction and Pairing Mechanism in Superconducting Ca-Intercalated Bilayer Graphene. *Sci. Rep.* **2016**, *6*, 21414.
- [25] Zheng, J. J.; Margine, E. R. First-principles Calculations of the Superconducting Properties in Li-decorated Monolayer Graphene within the Anisotropic Migdal-Eliashberg Formalism. *Phys. Rev. B* **2016**, *94*, 064509.
- [26] Zhang, R.; Waters, J.; Geim, A. K.; Grigorieva, I. V. Intercalant-Independent Transition Temperature in Superconducting Black Phosphorus. *Nat. Commun.* **2017**, *8*, 15036.
- [27] Huang, G. Q.; Xing, Z. W.; Xing, D. Y. Prediction of Superconductivity in Li-intercalated Bilayer Phosphorene. *Appl. Phys. Lett.* **2015**, *106*, 113107.
- [28] Guan, J.; Liu, D.; Zhu, Z.; Tománek, D. Two-Dimensional Phosphorus Carbide: Competition Between sp^2 and sp^3 Bonding. *Nano Lett.* **2016**, *16*, 3247-3252.
- [29] Wang, G.; Pandey, R.; Karna, S. P. Carbon Phosphide Monolayers with Superior Carrier Mobility. *Nanoscale* **2016**, *8*, 8819-8825.
- [30] Wang, Y.; Lv, J.; Zhu, L.; Ma, Y. Crystal Structure Prediction via Particle-Swarm Optimization. *Phys. Rev. B* **2010**, *82*, 094116.
- [31] Kresse, G.; Furthmüller, J. Efficient Iterative Schemes for Ab Initio Total-Energy Calculations Using A Plane-Wave Basis Set. *Phys. Rev. B* **1996**, *54*, 11169.
- [32] Tan, W. C.; Cai, Y.; Ng, R. J.; Huang, L.; Feng, X.; Zhang, G.; Zhang, Y. W.; Nijhuis, C. A.; Liu, X.; Ang, K. W. Few-Layer Black Phosphorus Carbide Field-Effect Transistor via Carbon Doping. *Adv. Mater.* **2017**, *29*, 1700503.
- [33] Rajbanshi, B.; Sarkar, P. Is the metallic phosphorus carbide (β_0 -PC) monolayer stable? An answer from a theoretical perspective. *J. Phys. Chem. Lett.* **2017**, *8*, 747-754.
- [34] N. Troullier and J. L. Martins, Efficient Pseudopotentials for Plane-Wave Calculations. *Phys. Rev. B* **1991**, *43*, 1993.
- [35] M. Fuchs and M. Scheffler, Ab Initio Pseudopotentials for Electronic Structure Calculations of Poly-Atomic Systems Using Density-Functional Theory. *Comput. Phys. Commun.* **1999**, *119*, 67-98.
- [36] Giannozzi, P.; Baroni, S.; Bonini, N.; Calandra, M.; Car, R.; Cavazzoni, C.; Ceresoli, D.; Chiarotti, G. L.; Cococcioni, M.; Dabo, I.; Dal Corso, A.; de Gironcoli, S.; Fabris, S.; Fratesi, G.; Gebauer, R.; Gerstmann, U.; Gougoussis, C.; Kokalj, A.; Lazzeri, M.; Martin-Samos, L.; Marzari, N.; Mauri, F.; Mazzone, R.; Paolini, S.; Pasquarello, A.; Paulatto, L.; Sbraccia, C.; Scandolo, S.; Sclauzero, G.; Seitsonen, A. P.; Smogunov, A.; Umari, P.; Wentzcovitch, R. M. QUANTUM ESPRESSO: A Modular and Open-Source Software Project for Quantum Simulations of Materials. *J. Phys.: Condens. Matter* **2009**, *21*, 395502.

- [37] S. Baroni, S. de Gironcoli, A. Dal Corso, and P. Gian-nozzi, Phonons and Related Crystal Properties from Density-Functional Perturbation Theory. *Rev. Mod. Phys.* **2001**, *73*, 515.
- [38] Langmuir, I. The Arrangement of Electrons in Atoms and Molecules. *J. Am. Chem. Soc.* **1919**, *41*, 868-934.
- [39] Song, Q.; Wang, B.; Deng, K.; Feng, X.; Wagner, M.; Gale, J. D.; Müllen, K.; Zhi, L. Graphenylene, a unique two-dimensional carbon network with nondelocalized cyclohexatriene units. *Journal of Materials Chemistry C* **2013**, *1*, 38-41.
- [40] Yu, Y. X. Graphenylene: a promising anode material for lithium-ion batteries with high mobility and storage. *Journal of Materials Chemistry A* **2013**, *1*, 13559-13566.
- [41] Wang, Z.; Zhou, X. F.; Zhang, X.; Zhu, Q.; Dong, H.; Zhao, M.; Oganov, A. R. Phagraphene: a low-energy graphene allotrope composed of 5-6-7 carbon rings with distorted dirac cones. *Nano lett.* **2015**, *15*, 6182-6186.
- [42] Zhu, Z.; Tománek, D. Semiconducting Layered Blue Phosphorus: A Computational Study. *Phys. Rev. Lett.* **2014**, *112*, 176802.
- [43] Guan, J.; Zhu, Z.; Tománek, D. Phase Coexistence and Metal-Insulator Transition in Few-Layer Phosphorene: A Computational Study. *Phys. Rev. Lett.* **2014**, *113*, 046804.
- [44] Özçelik, V. O.; Azadani, J. G.; Yang, C.; Koester, S. J.; Low, T. Band Alignment of Two-Dimensional Semiconductors for Designing Heterostructures with Momentum Space Matching. *Phys. Rev. B* **2016**, *94*, 035125.
- [45] Kresse, G.; Furthmüller, J. Efficiency of ab-initio total energy calculations for metals and semiconductors using a plane-wave basis set. *Comput. Mater. Sci.* **1996**, *6*, 15-50.
- [46] Soler, J. M.; Artacho, E.; Gale, J. D.; García, A.; Junquera, J.; Ordejo, P.; Saáchez-Portal, D. The SIESTA Method for ab initio Order-N Materials Simulation. *J. Phys.: Condens. Matter* **2002**, *14*, 2745.
- [47] Daly, J. J. The crystal and molecular structure of triphenylphosphorus. *J. Chem. Phys.* **1964**, *729*, 3799-3810.
- [48] Zhang, X.; Zhou, Y.; Cui, B.; Zhao, M.; Liu, F. Theoretical Discovery of a Superconducting Two-Dimensional Metal-Organic Framework. *Nano Lett.* **2017**, *17*, 6166-6170.
- [49] Kohn, W. Image of the Fermi Surface in the Vibration Spectrum of a Metal. *Phys. Rev. Lett.* **1959**, *2*, 393-394.
- [50] Caruso, F.; Hoesch, M.; Achatz, P.; Serrano, J.; Krisch, M.; Bustarret, E.; Giustino, F. Nonadiabatic Kohn Anomaly in Heavily Boron-Doped Diamond. *Phys. Rev. Lett.* **2017**, *119*, 017001.
- [51] Bardeen, J.; Cooper, L. N.; Schrieffer, J. R. Theory of Superconductivity. *Phys. Rev.* **1957**, *108*, 1175-1204.
- [52] McMillan, W. L. Transition Temperature of Strong-Coupled Superconductors. *Phys. Rev.* **1968**, *167*, 331-344.
- [53] Allen, P. B.; Dynes, R. C. Transition Temperature of Strong-Coupled Superconductors Reanalyzed. *Phys. Rev. B* **1975**, *12*, 905-922.
- [54] Penev, E. S.; Kutana, A.; Yakobson, B. I. Can Two-Dimensional Boron Superconduct? *Nano Lett.* **2016**, *16*, 2522-2526.
- [55] Cheng, C.; Sun, J. T.; Liu, H.; Fu, H. X.; Zhang, J.; Chen, X. R.; Meng, S. Suppressed superconductivity in substrate-supported β_{12} borophene by tensile strain and electron doping. *2D Mater.* **2017**, *4*, 025032.
- [56] Zhang, J. J.; Dong, S. Superconductivity of Monolayer Mo₂C: The Key Role of Functional Groups. *J. Chem. Phys.* **2017**, *146*, 034705.
- [57] Zhao, Y.; Zeng, S.; Ni, J. Superconductivity in Two-Dimensional Boron Allotropes. *Phys. Rev. B* **2016**, *93*, 014502.
- [58] Dai, J.; Li, Z.; Yang, J.; Hou, J. A First-Principles Prediction of Two-Dimensional Superconductivity in Pristine B₂C single layers. *Nanoscale* **2012**, *4*, 3032-3035.
- [59] Wu, Q.; Zhang, J. J.; Hao, P.; Ji, Z.; Dong, S.; Ling, C.; Chen, Q.; Wang, J. Versatile Titanium Silicide Monolayers with Prominent Ferromagnetic, Catalytic, and Superconducting Properties: Theoretical Prediction. *J. Phys. Chem. Lett.* **2016**, *7*, 3723-3729.
- [60] Wu, C.; Wang, H.; Zhang, J.; Gou, G.; Pan, B.; Li J. Lithium-Boron (Li-B) Monolayers: First-Principles Cluster Expansion and Possible Two-Dimensional Superconductivity. *ACS Appl. Mater. Interfaces* **2016**, *8*, 2526-2532.
- [61] Mannix, A. J.; Zhou, X. F.; Kiraly, B.; Wood, J. D.; Alducin, D.; Myers, B. D.; Liu, X.; Fisher, B. L.; Santiago, U.; Guest, J. R.; Yacaman, M. J.; Ponce, A.; Oganov, A. R.; Hersam, M. C.; Guisinger, N. P. Synthesis of Borophenes: Anisotropic, Two-Dimensional Boron Polymorphs. *Science* **2015**, *350*, 1513-1516.
- [62] Feng, B.; Zhang, J.; Zhong, Q.; Li, W.; Li, S.; Li, H.; Cheng, P.; Meng, S.; Chen, L.; Wu, K. Experimental Realization of Two-Dimensional Boron Sheets. *Nat. Chem.* **2016**, *8*, 563-568.
- [63] Xi, X.; Berger, H.; Forró, L.; Shan, J.; Mak, K. F. Gate Tuning of Electronic Phase Transitions in Two-Dimensional NbSe₂. *Phys. Rev. Lett.* **2016**, *117*, 106801.
- [64] Fu, Z. G.; Hu, Z. Y.; Yang, Y.; Lu, Y.; Zheng, F. W.; Zhang, P. Modulation of Doping and Biaxial Strain on The Transition Temperature of The Charge Density Wave Transition in 1T-TiSe₂. *RSC Adv.* **2016**, *6*, 76972.